

# Adversarial samples for deep monocular 6D object pose estimation

Jinlai Zhang<sup>1</sup>, Weiming Li<sup>2</sup>, Shuang Liang<sup>2</sup>, Hao Wang<sup>2</sup>, and Jihong Zhu<sup>1,3</sup>

<sup>1</sup> Guangxi University

<sup>2</sup> Samsung Research China - Beijing (SRC-B)

<sup>3</sup> Tsinghua University

**Abstract.** Estimating 6D object pose from an RGB image is important for many real-world applications such as autonomous driving and robotic grasping. Recent deep learning models have achieved significant progress on this task but their robustness received little research attention. In this work, for the first time, we study adversarial samples that can fool deep learning models with imperceptible perturbations to input image. In particular, we propose a Unified 6D pose estimation Attack, namely U6DA, which can successfully attack several state-of-the-art (SOTA) deep learning models for 6D pose estimation. The key idea of our U6DA is to fool the models to predict wrong results for object instance localization and shape that are essential for correct 6D pose estimation. Specifically, we explore a transfer-based black-box attack to 6D pose estimation. We design the U6DA loss to guide the generation of adversarial examples, the loss aims to shift the segmentation attention map away from its original position. We show that the generated adversarial samples are not only effective for direct 6D pose estimation models, but also are able to attack two-stage models regardless of their robust RANSAC modules. Extensive experiments were conducted to demonstrate the effectiveness, transferability, and anti-defense capability of our U6DA on large-scale public benchmarks. We also introduce a new U6DA-Linemod dataset for robustness study of the 6D pose estimation task. Our codes and dataset will be available at <https://github.com/cuge1995/U6DA>.

**Keywords:** Adversarial samples, 6 DoF pose estimation, robust model

## 1 Introduction

Understanding object pose in the three-dimensional world is an important research topic in computer vision. In the past decade, extensive research efforts have been made and achieved significant progress. In particular, recent deep learning based methods show that even using only a single RGB image without any additional depth data, 6D object pose can be predicted with high accuracy on large-scale public benchmarks [33,44,25]. Such monocular 6D object pose estimation models shed light on the possibility of single-RGB sensor based solutions for various 3D applications such as augmented reality [1,47], autonomous driving [28,29] and robotic grasping [43,11,41]. In these real-world scenarios, model

robustness is a crucial issue to consider. In some recent research, deep learning models are found to be vulnerable to adversarial samples [5,6] in 2D image classification task. The adversarial samples contain human imperceptible perturbations to the input and can result wrong model prediction. Does such problem apply to other tasks? Inspired by such concerns, to the best of our knowledge, this work for the first time studies adversarial samples for the monocular 6D object pose estimation task. To mention, our discussion is focused on instance-level 6D object pose estimation with known object 3D models. Some other works study category-level object pose estimation for unseen objects, which are beyond the scope of this paper’s discussion.

Following the conventions in literature, SOTA deep learning methods for 6D object pose estimation can be roughly divided into three classes: direct methods, key-point based methods and dense coordinate based methods. The latter two classes follow two-stage scheme. The direct methods [44,46] directly output pose parameters from the input RGB image. With two-stage scheme, the key-point based methods [33] use DNN models to detect 2D keypoints in the image first, and then solve a RANSAC-based Perspective-n-Point (PnP) problem [24] for 6D pose estimation. The dense coordinate based methods [25] use DNNs to build dense 2D-3D correspondences, and then estimate 6D pose by solve RANSAC-based PnP problem. Recent research results on public benchmark show that all the top-performing algorithms follow the two stage scheme. It’s noticeable that the two-stage schemes include RANSAC-based PnP that are known to be robust to noise. Meanwhile, the un-differentiable part of RANSAC-based PnP makes it impossible to implement white-box attack [8]. These features indicate that a direct application of straight-forward adversarial attack methods may not work for these models.

Based on an observation that all the three classes of methods rely on object instance localization and shape, we infer that the adversarial samples crafted by attacking a segmentation task could be likely to transfer to 6D pose estimation task. To this end, we propose a Unified 6D pose estimation Attack, namely U6DA, which can successfully attack all the three classes of deep learning models for 6D pose estimation. Specifically, we explore a transfer-based black-box attack to 6D pose estimation, and we select the segmentation model as surrogate model. We design the U6DA loss to guide the generation of adversarial examples, the loss aims to shift the segmentation attention map away from its original position.

We perform extensive experimental evaluations on the proposed U6DA on both the Linemod [14] and Linemod Occlusion [2] dataset. Compared to two straight forward task-transfer attack methods [27] [6], we show that our U6DA is much more effective to 6D pose estimation attack. We also show the transferability of our U6DA attack. The adversarial samples generated by our U6DA can significantly decrease the ADD metric of all three mainstream RGB-based 6D pose estimation networks. In addition, we make two extension studies. We first examine whether the SOTA physically-based rendering [18] (PBR) training is more robust than normal training. Our experimental results show that the PBR training is not as robust as normal training. Second, we demonstrate that

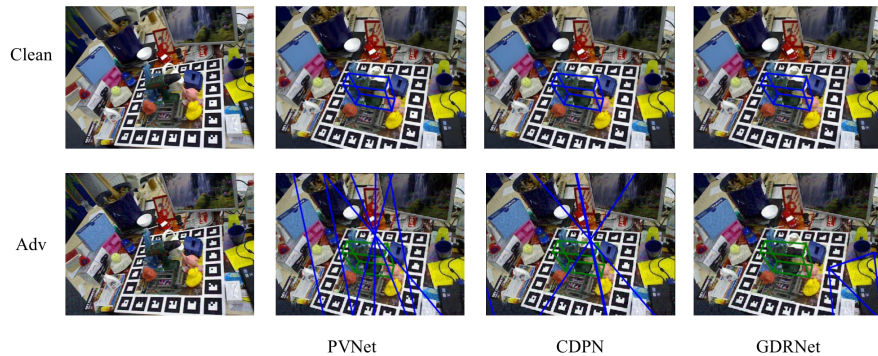


Fig. 1: Comparison of pose estimation results with clean image and our U6DA generated adversarial image as inputs respectively. Column one shows a clean image and its adversarial image crafted by our U6DA. They are input to three deep learning models [33,44,25] of different methodologies, and their estimated poses for an object instance (driller in LINEMOD dataset) are shown in column 2-4. In each image, green and blue box denote ground truth and the predicted pose respectively. All the three deep models predict wrong poses with the adversarial image, which shows our U6DA attack is successful.

the RGB-D based 6D pose estimation networks are more robust to RGB adversary. We also perform experiments to test classical adversarial defense algorithms and show that they are less effective on our U6DA. Finally, we introduce a new U6DA-Linemod dataset for robustness test of 6D pose estimation task, which we hope will benefit the 6D pose estimation community. In summary, the major contributions of this work are as follows:

1. A novel adversarial attack method U6DA is proposed that is effective for several classes of SOTA deep learning models for 6D object pose estimation.
2. Extensive experiments are performed to examine the effectiveness, transferability, anti-defense capability of the U6DA method on large scale public benchmark datasets.
3. We construct a public-available U6DA-Linemod dataset for robustness test of 6D pose estimation models.

## 2 Related work

### 2.1 Adversarial attacks

Adversarial attack [8] refers to the process of applying a slight perturbation to the original input of deep learning model to generate adversarial samples that fool the target model (also known as the victim model). Adversarial attack methods have been extensively studied in the image classification task [5,6,44]. Most of them are in the white-box setting, where full-knowledge of the DNN is known by the attacker. However, white-box attacks are not practical for many real

applications where the attacker only knows the output of networks. Therefore, the black-box attacks where the attacker has no prior knowledge or only partial knowledge of the model are getting more research attentions. Recently, there are also some works focus on 3D point clouds [26] and 3D meshes [48]. However, to the best of our knowledge, there is no adversarial attack to the 6D pose estimation task. In this paper, we make discussions to explore the black-box attack to 6D pose estimation task.

## 2.2 6D pose Estimation with RGB image

Following the conventions in literature, SOTA deep learning methods for monocular 6D object pose estimation with one RGB image can be roughly divided into three classes: direct methods, key-point based methods and dense coordinate based methods. Next, we give a brief review for each class of methods respectively.

**Direct methods.** These methods directly forecast the 6D object pose from input image, which treat the 6D pose estimation as a regression or classification task. Xiang et al. [46] propose PoseCNN, a novel end-to-end 6D pose estimation model, which decouples 6D pose estimation task into several different components. For the translation branch, it firstly localizes the object center in the image and estimates the depth with respect to the camera. Then the translation is recovered according to the projection equation. The rotation is regressed a quaternion representation directly. Instead of regressing rotation directly, SSD-6D [22] treats rotation estimation as a classification problem via broken down the rotation space into classifiable ranges. Recently, researchers[44,19] aim at mapping the Perspective-n-Point [24] (PnP) algorithm using DNNs. For instance, the GDRNet [44] predicts the 6D pose via a Patch-PnP solver that is built upon DNNs. However, the DNNs are known to be vulnerable to adversarial attacks [8], it would be interesting to explore whether the direct methods are robust to adversarial samples.

**Key-point based methods.** The keypoint-based methods are generally more accurate compared to the direct methods. It usually uses DNNs to detect 2D keypoints in the image and then follow a Perspective-n-Point (PnP) solver to get the 6D pose. BB8 [35] firstly uses DNNs to segment the target object and then builds 2D-3D correspondences via another DNN. Then the 6D pose can be estimated by a PnP solver. YOLO-6D [40] uses the YOLO backbone to detect the 2D key-point of 3D bounding box corners, followed by a PnP solver to forecast 6D pose. [30] predicts the 2D projections of 3D keypoints via a 2D heatmaps. PVNet [33] is built upon the idea of voting-based key-point localization. It first trains DNNs to regress pixel-wise vectors pointing to the key-points, and then uses the vectors to vote for key-point locations. The PVNet yields pretty good performance under severe occlusion or truncation due to this vector-field representation. We therefore select PVNet as a victim model as a representative of key-point based method to test our attacks.

**Dense coordinate based methods.** The dense coordinate based methods solve the 6D pose estimation task via building dense 2D-3D correspondences, followed by a PnP solver to estimate the 6D pose. The dense 2D-3D correspondences are built via forecasting the 3D object coordinate of each target object pixel. CDPN [25] firstly using DNNs for dense coordinates forecasting. Pix2Pose [31] proposes a transformer loss to handle symmetric objects, thus improving the performance of 6D pose estimation of symmetric objects significantly compared to CDPN. In this paper, we select the CDPN as a victim model that represents the dense coordinate based methods.

### 2.3 Dataset for 6D Pose Estimation

There exist many datasets for 6D pose estimation. The Linemod[14] is the classical benchmark for instance-level 6D object pose estimation. Linemod Occlusion [2] is a variant of Linemod that makes up for Linemod that it lacks occlusion cases. In most papers [44,33], Linemod Occlusion is used for testing DNNs trained on Linemod. The YCB video [46] is bigger than Linemod, it consists of 21 objects collected from YCB object set [4]. And the various lighting conditions, severe occlusions make it much more challenging than Linemod. The T-LESS [15] aims to push the limit of 6D object pose estimation with texture-less objects. The HomebrewedDB [21] focus on household objects and low-textured industrial objects. The above datasets are mainly focused on occlusion and texture-less of objects. It can be seen that, compared to ImageNet variants [13] in the field of image classification, a large-scale public dataset to evaluate the algorithm robustness is absent in the field of 6D object pose estimation.

## 3 Methodology

In this section, we introduce our U6DA algorithm. Given an RGB image, the U6DA generates an adversarial perturbation that aims at confusing deep 6D pose estimation networks.

### 3.1 Problem Definition

In this paper, we focus on the adversarial attacks on instance level monocular 6D pose estimation. Given an RGB image  $I$ , our goal is to generate an adversarial image  $I_{adv}$  that can fool deep learning models of 6D pose estimation. Firstly, we give a brief introduction of deep 6D pose estimation from RGB image. The deep 6D pose estimation networks aim to estimate the object pose of the target instance when given an RGB image  $I$  and the target 3D model  $\mathcal{M}$ . The 6D pose can be represented as rotation  $\mathcal{R} \in SO(3)$  and translation  $\mathcal{T} \in R^3$  w.r.t the camera. The whole task can be described as follows:

$$[\mathcal{R}|\mathcal{T}] = F\{I, \mathcal{M}|\theta\} \quad (1)$$

---

**Algorithm 1** Unified 6D Pose Estimation Attack (U6DA) to fool deep 6D pose estimation networks.

---

**Input:** Original RGB image  $I$ , trained UNet model  $\mathcal{F}_\theta()$ , perturbation clipping factor  $\epsilon$ , max iteration  $M$ .

**Output:** Perturbed RGB image  $I_{adv}$ .

- 1: set initial  $I_{adv}^0 = I, g_0 = 0, \alpha = \epsilon/M$
- 2:  $\{Calculate\ attention\ map\ M_{ori}\ of\ I_{adv}^0\}$  ▷ Eq. 4
- 3: get shifted attention map  $M_{sh}$
- 4: **while**  $i < M$  **do**
- 5:    $\{Calculate\ attention\ map\ M_{adv}\ of\ I_{adv}^i\}$  ▷ Eq. 4
- 6:    $g^i = \frac{\partial L_{u6da}(M_{adv} - M_{sh})}{\partial I_{adv}^i}$
- 7:    $g^{i+1} = g^i + \frac{g^i}{\|g^i\|_1}$
- 8:    $I_{adv}^{i+1} = clip_\epsilon(I_{adv}^i - \alpha * sign(g^{i+1}))$
- 9:    $i = i + 1$
- 10: **end while**
- 11: **return**  $I_{adv}^i$

---

where  $F$  refers to a specific deep 6D pose estimation network, and  $\theta$  refers to the network’s parameters. We aim to generate an adversarial example  $I^{adv} = I + \epsilon$ , which is distorted by carefully designed perturbation  $\epsilon$  but will mislead the 6D pose estimation network. Typically,  $\ell_p$ -norm is commonly adopted to regularize the perturbation. Here, we define the generation of adversarial examples in the following.

$$\arg \min_{I^{adv}} ADD, \text{ s.t. } \|I - I^{adv}\|_p \leq \epsilon, \quad (2)$$

where the  $ADD$  is pose accuracy metric following the definition in [16,14], and  $p = \infty$  in this paper. Owing to two stage scheme of deep 6D pose estimation networks, it is impossible to solve the above problem via the famous Fast Gradient Sign Method [9] (FGSM) or other white-box attacks. Instead, inspired by [20], we generate adversarial examples via transfer-based attack.

### 3.2 Unified 6D Pose Estimation Attack

The overall framework of our Unified 6D Pose Estimation Attack (U6DA) is shown in Algorithm 1. The U6DA generates adversarial examples via a pre-trained segmentation network. The intuition of our U6DA is simple, since the deep 6D pose estimation networks heavily rely on the semantic segmentation information of the target instance to localize the object, we infer that an attack on the segmentation network could transfer to the deep 6D pose estimation network. Therefore, we use the classical segmentation network UNet [36] as our surrogate model.

To pursue high transferability of U6DA to three mainstream deep 6D pose estimation networks, we need to find common features of those networks. Inspired by [20] and the analysis in the previous section, we firstly select deep segmentation networks to learn the general features. Moreover, we attack on the

attention map to avoid overfitting in the segmentation task and fool the models to predict wrong results for object shapes that are essential for correct 6D pose estimation. Specifically, we design the U6DA loss to guide the generation of adversarial examples, the loss aims to shift the segmentation attention map away from its original position. The key idea of our U6DA is if we shift the general features away from their original position, the following RANSAC-based PnP solver would make wrong estimation.

Next, we describe U6DA step by step. We use the Seg Grad CAM [42] as the attention map due to its impressive performance in explaining segmentation networks. We therefore first introduce the Grad CAM [37] and Seg Grad CAM [42] as follows:

**Grad CAM.** The Grad CAM is designed for explain the classification models, which is calculated as follows:

$$M^c = \text{ReLU}\left(\sum_k \alpha_c^k A^k\right) \quad \text{with} \quad \alpha_c^k = \frac{1}{N} \sum_{u,v} \frac{\partial y^c}{\partial A_{uv}^k} \quad (3)$$

where  $\{A^k\}_{k=1}^K$  is a set of selected feature maps of interest ( $K$  kernels of the last convolutional layer of a classification network), and  $y^c$  is the logit for a chosen class  $c$ . Grad-CAM averages the gradients of  $y^c$  with respect to all  $N$  pixels (indexed by  $u, v$ ) of each feature map  $A^k$  to produce a weight  $\alpha_c^k$  to denote its importance.

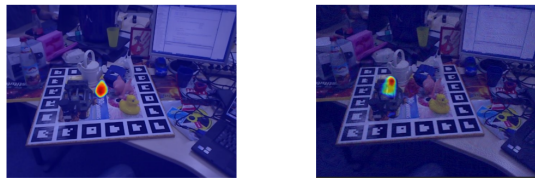
**Seg Grad CAM.** The Seg Grad CAM is the extension of Grad CAM that can interpretation of segmentation problems. It is defined as follows:

$$M_{seg}^c = \text{ReLU}\left(\sum_k \alpha_c^k A^k\right) \quad \text{with} \quad \alpha_c^k = \frac{1}{N} \sum_{u,v} \frac{\partial \sum_{(i,j) \in \mathcal{M}} y_{ij}^c}{\partial A_{uv}^k} \quad (4)$$

where  $\mathcal{M}$  is a set of pixel indices of interest in the output mask.

Let  $M_{seg}^t$  stand for the attention map for the input  $I$  and a specified class  $t$ . We push the attention map away from its original position. Therefore, our loss would be:

$$L_{u6da}(I) = \|M_{adv} - M_{sh}\|_1 \quad (5)$$



Original

Adv

Fig. 2: Attention map visualization of clean image and adversarial image. The attention map of adversarial image is away from its original position.

where the  $M_{adv}$  is the attention map from the adversarial sample, the  $M_{sh}$  is the shifted attention map from the clean sample.

The adversarial samples are generated in an update process guided by the U6DA loss  $L_{u6da}$ . As shown in Algorithm 1, we set  $I_{adv}^0 = I$  and the update it by momentum iterative method [6]. Followed previous works [8,6], we restrict our attack via the  $\ell_\infty$  distance.

Because its attention maps have shifted away from the original position, U6DA could be used for the black-box attack to the mainstream 6D pose estimation networks. Due to the RANSAC-based PnP solver could be affected by our U6DA, the generated adversarial samples tend to be aggressive to the mainstream 6D pose estimation networks.

## 4 Experimental Results

### 4.1 Experimental settings

**Dataset and models.** **Linemod** [14] consists of 13 RGBD sequences, and the ground-truth 6D poses of each object are provided for each sequences. The image size is  $640 \times 480$ . Following previous studies [44,33], we select 15% of images of each sequence for training and the remaining 85% for testing. Note that of the RGBD images, we use only the RGB images as input. **Linemod Occlusion** [2] is generated from Linemod dataset, and it was generally used for test the performance of 6D pose estimation networks under occlusion conditions. We use Linemod and Linemod Occlusion dataset. Three SOTA models are selected as the target model, which are the GDRNet [44], PVNet [33], CDPN [25]. For segmentation networks, we use Pytorch to build the segmentation networks, such as Unet [36], Unet++ [49], FPN [23], DeepLabV3 [7].

**Metrics.** We use the ADD metric as our evaluation metric. Following the definition in [16,14], if the distance is less than 10% of the model’s diameter, we suppose the estimated pose is correct.

**Implementation details.** We implement our U6DA attack in Pytorch [32], the perturbation size is  $\epsilon = 16$  for all experiments with pixel values in  $[0, 255]$  and the attack steps is 5. We train the segmentation models based on Pytorch using ResNet34 [10] as encoder, the training set is from Linemod. The epoches of training is 40, in the first 25 epoches, the learning rate is 0.001, and the later epoches are with a learning rate 0.00001.

### 4.2 Sensitivity analysis

Here, we conduct a series of experiments on Linemod dataset to analyze the following aspects of our U6DA. All the attacks are implemented on benchvise instance to PVNet.



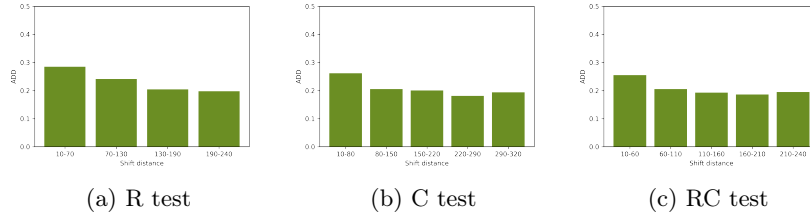


Fig. 3: The effect of different shift distance.

**Shift Position.** In our U6DA attack, we shift the attention map away from its original position and this leads to error in the RANSAC-based PnP solver. In this section, we explore the effect of different shift position on U6DA. In Linemode dataset, the image size is 640 pixels in width and 480 pixels in height, and most objects are located at image center. We therefore firstly perform a shift in the up and down direction of height with the maximum shift distance as half of the height (R test), and then perform shift in the left and right direction of width with the maximum shift distance as half of the width (C test). Lastly, we perform shift in both width and height (RC test). For R test, we first randomly select the up or down direction, and the shift distance is randomly generated within a certain range. We perform four different sets of experiments with shift distance 10-70, 70-130, 130-190, 190-240. For R test, we first randomly select the left or right direction, then the shift distance is randomly selected from 10-80, 80-150, 150-220, 220-290, 290-320. For RC test, both shift directions are generated followed R test and C test, the shift distance is randomly selected from 10-60, 60-110, 110-160, 160-210, 210-240. The experimental results are shown in Figure 3 a,b,c. It can be seen that the width shift is more effective for U6DA. In order to avoid overfitting to PVNet, we select width and height shift with 110-160 shift distance in the following experiments.

**The effect of different segmentation models.** Since our U6DA attack is firstly performed on the segmentation model and then transfer to the 6D pose estimation models, in this section we explore the effect of different segmentation models on the transferability. We perform U6DA attack on the Unet [36], Unet++ [49], FPN [23], DeepLabV3 [7] and their ensembles. The results are shown in Table 1, the ensemble attack might increase the attack performance but requires much more computing resources. Unlike the adversarial attack of image classification that ensemble victim model will improve the transferability considerably [6], our ensembled models do not always bring a performance improvement. For example, the combination of all models achieves relatively poor performance. Moreover, although the DeepLabV3 achieved the best attack performance over single model, it was slower than Unet, the DeepLabV3 needs 3.24s in every iteration of our U6DA attack while Unet only needs 0.08s in NVIDIA RTX 3090 GPU, we therefore select the Unet as our surrogate model in the following experiments.

Table 1: The ADD of our U6DA attack based on different segmentation models. The clean ADD is 99.52.

Victim models	ADD
UNet	19.65
UNet++	46.12
FPN	28.19
DeepLabV3	<b>16.27</b>
UNet + UNet++	20.63
UNet + FPN	25.48
UNet + DeepLabV3	23.93
FPN + UNet++	22.48
DeepLabV3 + UNet++	<b>19.57</b>
FPN + DeepLabV3	26.06
UNet + FPN + UNet++	<b>14.92</b>
UNet + DeepLabV3 + UNet++	36.82
UNet + FPN + DeepLabV3	21.70
FPN + DeepLabV3 + UNet++	27.13
UNet + FPN + DeepLabV3 + UNet++	40.69

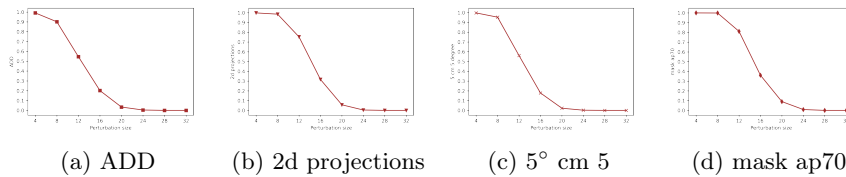


Fig. 4: The effect of different perturbation size.

**The effect of different perturbation size.** In the adversarial attack on image domain, the  $\epsilon = 16$  is a commonly used attack strength that generally considered imperceptible to humans [5,6,20,45]. To gain a deep understanding of U6DA attack, we also performed attacks with  $\epsilon$  in [4,8,12,16,20,24,28,32]. As shown in Figure 4, when  $\epsilon > 20$ , the ADD decreased to almost zero. We also present the 2D Projection metric [3], 5° 5 cm [39] and mask ap70 [33], those metrics are dropped sharply from 4 to 16, and then reach almost 0 when  $\epsilon > 20$ .

### 4.3 Comparasion with SOTA cross task attack.

Our U6DA transfer the adversarial examples from segmentation models to the 6D pose estimation models, which is a cross task attack. We therefore compare our U6DA with SOTA cross task attack, the DR attack [27], which aims to reduce the standard deviation of internal feature map. We also compare a strong transferable attack, MI-FGSM [6]. We perform DR and MI-FGSM attack on the Unet, which is the same as our U6DA.

As shown in Table 2, our U6DA outperform DR and MI-FGSM attack significantly when transfered to PVNet. We infer that due to the 6D pose estimation

Table 2: The ADD of our U6DA compared to the SOTA corss task attack. The clean denotes the clean data.

Victim model	clean	U6DA attack	DR attack	MI-FGSM
PVNet	99.52	<b>19.65</b>	91.18	51.93

Table 3: The ADD of clean data and adversarial samples of three mainstream RGB based deep 6D pose estimation networks on the **LINEMOD** dataset. The clean denotes the clean data, the adv denotes the adversarial attack generated by our U6DA.

Models	GDRNet		CDPN		PVNet	
	clean	adv	clean	adv	clean	adv
data						
ape	76.29	0.00	64.67	0.13	47.71	4.09
benchwise	97.96	3.98	96.80	37.21	99.52	19.65
cam	95.29	0.00	90.69	3.93	84.21	0.98
can	98.03	0.00	94.78	14.54	95.86	35.62
cat	93.21	0.00	85.53	2.91	77.64	17.76
driller	97.72	0.00	92.37	0.13	96.53	0.19
duck	80.28	0.00	66.76	0.64	55.96	10.79
eggbox	99.53	0.00	99.53	5.63	100	31.45
glue	98.94	0.00	98.75	6.51	81.27	17.86
holepuncher	91.15	0.00	87.44	4.24	81.16	24.17
iron	98.06	0.51	95.61	34.72	98.47	41.47
lamp	99.14	0.00	96.26	19.01	99.42	10.75
phone	92.35	0.00	85.84	13.99	91.74	27.08
average	93.69	0.35	88.85	11.05	85.34	18.60

based on DNNs having a different paradigm from the classification, segmentation and object detection task, the DR attack can have high transferability between the later tasks, but have relatively lower transferability on the 6D pose estimation task.

#### 4.4 Transferability Results

In this section, we perform U6DA to three mainstream RGB based deep 6D pose estimation networks, which are the direct methods GDRNet [44], the key-point based methods PVNet [33], the dense coordinate based methods CDPN [25]. The results of U6DA are shown in Table 3. The direct methods GDRNet are the most vulnerable to U6DA attack among three models. We infer that might be caused by the Linear Behavior [8] of deep networks, the direct methods directly output the 6D pose from an input RGB image, a small perturbation to the input is enough to make the prediction result very biased. As for the dense coordinate based methods CDPN, which was not as robust as the key-point based methods PVNet. The ADD of all instance and networks are decreased significantly, which validate the effectiveness of our U6DA attack.

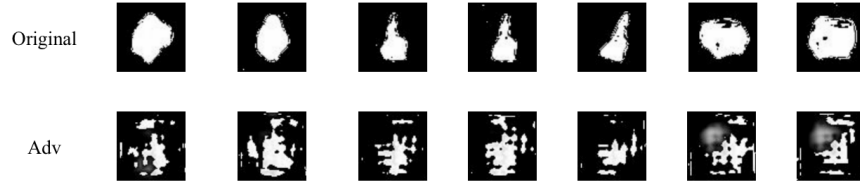


Fig. 5: Visualization of the Visible Object Mask of GDRNet.



Fig. 6: Visualization of the vector field map (bottom row) and segmentation mask (top row) of PVNet.

We also explore how U6DA works for PVNet and GDRNet. We visualized the vector field map and segmentation mask of PVNet with both clean sample and adversarial sample. The benchvise and cat instance are presented. For GDRNet, we randomly select some Visible Object Mask of clean samples and adversarial samples craft by our U6DA. From Figure 5 and Figure 6, we can observed that the Visible Object Mask of adversarial sample is relatively messy compared to the clean sample, the intermediate representation of PVNet has moved and slightly deformed after U6DA attack. Overall, the intermediate representation of PVNet is much robust than GDRNet, this might be the reason why PVNet is more robust than GDRNet under our U6DA.

#### 4.5 U6DA under defense

We also evaluate our U6DA attack under several adversarial defenses, such as JPEG compression [38] and pixel deflection [34] (PD). The results are shown in Table 4. The PD defense slightly increased the ADD, but the JPEG compression defense decreased the ADD significantly. The results indicated that the traditional denoising-based defense is ineffective to our U6DA attack.

#### 4.6 Extension studies

**Are PBR trained model more Robust?** The physically-based rendering[18] (PBR) training are dominated in RGB-based 6D pose estimation to improve the

Table 4: The ADD of our U6DA attack under adversarial defenses. The instance is benchvise of Linemod dataset.

Victim model	U6DA	JPEG	PD
PVNet	19.65	1.74	20.25

Table 5: The ADD of clean data and U6DA attack of GDRNet [44] on the **LINEMOD Occlusion** dataset. Where adv16 denotes adversarial samples generated with  $\epsilon = 16$  and adv8 denotes adversarial samples generated with  $\epsilon = 8$ .

Models	Real+Syn			Real+Pbr		
	clean	adv16	adv8	clean	adv16	adv8
ape	41.28	1.03	16.67	44.87	0.09	6.32
can	71.09	17.98	50.54	79.70	1.41	24.94
cat	18.20	0.08	1.35	30.58	0.08	0.51
driller	54.61	0.16	5.27	67.79	0.49	0.82
duck	41.64	20.03	26.95	39.98	4.72	17.24
eggbox	40.22	3.93	18.53	49.87	14.86	15.80
glue	59.49	27.19	50.28	73.70	20.31	48.72
holepuncher	52.56	6.12	29.59	62.73	1.57	23.88
average	47.39	9.57	24.89	56.15	5.44	17.28

accuracy and robustness, one intriguing question would be: are PBR trained model robust to adversarial attacks? To answer this question, we performed U6DA attack on GDRNet[44] with two  $\epsilon$  and two versions of GDRNet: One trained with real data from Linemod and synthetic images followed[33], another one is trained with real data and PBR data. As shown in Table 5, the answer is counterintuitive, the PBR doesn't improve the robustness to adversarial attack by our U6DA, instead, the robustness of real+synthetic training is consistently and significantly outperform the real+pbr training.

**Are RGB-D based deep 6D pose estimation networks robust to RGB adversary?** The RGB-D based methods are dominated in the BOP benchmark [17]. One interesting question would be are RGB-D based deep 6D pose estimation networks robust to RGB adversary? To answer this, we validate in Linemod dataset. We perform U6DA attack on FFB6D [11], PVN3D [12] and DenseFusion [43]. The results are shown in Table 6, we can observe that the RGB-D based deep 6D pose estimation networks are more robust to RGB adversary compared to the RGB based deep 6D pose estimation networks, the ADD of RGB-D models only slightly affected by RGB adversary.

#### 4.7 U6DA-Linemod dataset

In this section, we introduce U6DA-Linemod dataset. Following the BOP benchmark [18], we use U6DA to attack Unet to generate adversarial samples from

Table 6: The ADD of clean data and U6DA attack of three famous RGB-D based deep 6D pose estimation networks on the **LINEMOD** dataset. The clean denotes the clean data, the adv denotes the adversarial attack generated by our U6DA attack.

Models	FFB6D		PVN3D		DenseFusion	
	clean	adv	clean	adv	clean	adv
ape	98.76	51.71	97.23	95.61	93.42	92.37
benchwise	100.0	100.0	99.61	99.41	93.89	93.79
cam	100.0	70.88	99.60	84.11	97.35	95.98
can	99.90	99.50	99.40	97.54	94.19	93.79
cat	99.90	90.31	99.80	93.81	96.91	96.91
driller	100.0	90.78	99.30	49.85	87.41	84.84
duck	98.87	98.12	98.12	96.71	92.86	93.15
eggbox	100.0	95.86	99.81	98.21	99.81	99.81
glue	99.90	96.23	99.61	99.03	99.81	99.90
holepuncher	100.0	74.21	99.90	98.47	93.24	91.53
iron	100.0	99.89	99.69	99.28	97.96	98.06
lamp	100.0	95.49	99.81	98.08	96.55	96.45
phone	99.80	99.90	99.32	99.51	96.06	95.67
average	99.78	89.45	99.32	93.05	95.34	94.79

all the Linemod test set, we name this dataset as U6DA-Linemod. This dataset could be used for evaluating the robustness of SOTA 6D pose estimation models, and the adversarial defenses for 6D pose estimation also could benefit from it. The U6DA-Linemod can be download online, and by replacing the original BOP Linemod test set, the robustness of SOTA 6D pose estimation models could be evaluated.

## 5 Conclusion

In this paper, we propose U6DA, the first adversarial attack to deep 6D pose estimation networks. Our U6DA selects a segmentation model as surrogate model and then crafts adversarial samples by shifting the attention map. Extensive experiments reveal that the U6DA method is effective to fool all the three mainstream classes of 6D pose estimation networks with high transferability. Various experiments are performed to show properties of the U6DA such as parameter selection and effectiveness against data augmentation. Further more, we introduce a new U6DA-Linemod dataset, the first dataset on 6D pose estimation task to evaluate the robustness and defenses. In the future, we plan to explore how to systematically improve pose estimation model’s robustness against adversarial samples such as those generated by the U6DA.

## References

1. Barros, J.M.D., Mirbach, B., Garcia, F., Varanasi, K., Stricker, D.: Fusion of key-point tracking and facial landmark detection for real-time head pose estimation. In: 2018 IEEE Winter Conference on Applications of Computer Vision (WACV). pp. 2028–2037. IEEE (2018)
2. Brachmann, E., Krull, A., Michel, F., Gumhold, S., Shotton, J., Rother, C.: Learning 6d object pose estimation using 3d object coordinates. In: European conference on computer vision. pp. 536–551. Springer (2014)
3. Brachmann, E., Michel, F., Krull, A., Yang, M.Y., Gumhold, S., et al.: Uncertainty-driven 6d pose estimation of objects and scenes from a single rgb image. In: Proceedings of the IEEE conference on computer vision and pattern recognition. pp. 3364–3372 (2016)
4. Calli, B., Singh, A., Walsman, A., Srinivasa, S., Abbeel, P., Dollar, A.M.: The ycb object and model set: Towards common benchmarks for manipulation research. In: 2015 international conference on advanced robotics (ICAR). pp. 510–517. IEEE (2015)
5. Dong, Y., Fu, Q.A., Yang, X., Pang, T., Su, H., Xiao, Z., Zhu, J.: Benchmarking adversarial robustness on image classification. In: Proceedings of the IEEE/CVF Conference on Computer Vision and Pattern Recognition. pp. 321–331 (2020)
6. Dong, Y., Liao, F., Pang, T., Su, H., Zhu, J., Hu, X., Li, J.: Boosting adversarial attacks with momentum. In: Proceedings of the IEEE conference on computer vision and pattern recognition. pp. 9185–9193 (2018)
7. Florian, L.C., Adam, S.H.: Rethinking atrous convolution for semantic image segmentation. In: Conference on Computer Vision and Pattern Recognition (CVPR). IEEE/CVF (2017)
8. Goodfellow, I.J., Shlens, J., Szegedy, C.: Explaining and harnessing adversarial examples. arXiv preprint arXiv:1412.6572 (2014)
9. Goodfellow, I.J., Shlens, J., Szegedy, C.: Explaining and harnessing adversarial examples. In: Proceedings of International Conference on Learning Representations (ICLR) (2015), <http://arxiv.org/abs/1412.6572>
10. He, K., Zhang, X., Ren, S., Sun, J.: Deep residual learning for image recognition. In: Proceedings of the IEEE conference on computer vision and pattern recognition. pp. 770–778 (2016)
11. He, Y., Huang, H., Fan, H., Chen, Q., Sun, J.: Ffb6d: A full flow bidirectional fusion network for 6d pose estimation. In: Proceedings of the IEEE/CVF Conference on Computer Vision and Pattern Recognition. pp. 3003–3013 (2021)
12. He, Y., Sun, W., Huang, H., Liu, J., Fan, H., Sun, J.: Pvn3d: A deep point-wise 3d keypoints voting network for 6dof pose estimation. In: Proceedings of the IEEE/CVF conference on computer vision and pattern recognition. pp. 11632–11641 (2020)
13. Hendrycks, D., Dietterich, T.: Benchmarking neural network robustness to common corruptions and perturbations. In: International Conference on Learning Representations (2018)
14. Hinterstoisser, S., Lepetit, V., Ilic, S., Holzer, S., Bradski, G., Konolige, K., Navab, N.: Model based training, detection and pose estimation of texture-less 3d objects in heavily cluttered scenes. In: Asian conference on computer vision. pp. 548–562. Springer (2012)
15. Hodan, T., Haluza, P., Obdržálek, Š., Matas, J., Lourakis, M., Zabulis, X.: T-less: An rgb-d dataset for 6d pose estimation of texture-less objects. In: 2017 IEEE

- Winter Conference on Applications of Computer Vision (WACV). pp. 880–888. IEEE (2017)
16. Hodaň, T., Matas, J., Obdržálek, Š.: On evaluation of 6d object pose estimation. In: European Conference on Computer Vision. pp. 606–619. Springer (2016)
  17. Hodan, T., Michel, F., Brachmann, E., Kehl, W., GlentBuch, A., Kraft, D., Drost, B., Vidal, J., Ihrke, S., Zabulis, X., et al.: Bop: Benchmark for 6d object pose estimation. In: Proceedings of the European Conference on Computer Vision (ECCV). pp. 19–34 (2018)
  18. Hodaň, T., Sundermeyer, M., Drost, B., Labbé, Y., Brachmann, E., Michel, F., Rother, C., Matas, J.: Bop challenge 2020 on 6d object localization. In: European Conference on Computer Vision. pp. 577–594. Springer (2020)
  19. Hu, Y., Fua, P., Wang, W., Salzmann, M.: Single-stage 6d object pose estimation. In: Proceedings of the IEEE/CVF conference on computer vision and pattern recognition. pp. 2930–2939 (2020)
  20. Ilyas, A., Santurkar, S., Tsipras, D., Engstrom, L., Tran, B., Madry, A.: Adversarial examples are not bugs, they are features. In: Proceedings of the 33rd International Conference on Neural Information Processing Systems. pp. 125–136 (2019)
  21. Kaskman, R., Zakharov, S., Shugurov, I., Ilic, S.: Homebreweddb: Rgb-d dataset for 6d pose estimation of 3d objects. In: Proceedings of the IEEE/CVF International Conference on Computer Vision Workshops. pp. 0–0 (2019)
  22. Kehl, W., Manhardt, F., Tombari, F., Ilic, S., Navab, N.: Ssd-6d: Making rgb-based 3d detection and 6d pose estimation great again. In: Proceedings of the IEEE international conference on computer vision. pp. 1521–1529 (2017)
  23. Kirillov, A., He, K., Girshick, R., Dollár, P.: A unified architecture for instance and semantic segmentation (2017)
  24. Lepetit, V., Moreno-Noguer, F., Fua, P.: Epnp: An accurate o (n) solution to the pnp problem. *International journal of computer vision* **81**(2), 155 (2009)
  25. Li, Z., Wang, G., Ji, X.: Cdpn: Coordinates-based disentangled pose network for real-time rgb-based 6-dof object pose estimation. In: Proceedings of the IEEE/CVF International Conference on Computer Vision. pp. 7678–7687 (2019)
  26. Liu, B., Zhang, J., Chen, L., Zhu, J.: Boosting 3d adversarial attacks with attacking on frequency. *arXiv preprint arXiv:2201.10937* (2022)
  27. Lu, Y., Jia, Y., Wang, J., Li, B., Chai, W., Carin, L., Velipasalar, S.: Enhancing cross-task black-box transferability of adversarial examples with dispersion reduction. In: Proceedings of the IEEE/CVF Conference on Computer Vision and Pattern Recognition. pp. 940–949 (2020)
  28. Manhardt, F., Arroyo, D.M., Rupperecht, C., Busam, B., Birdal, T., Navab, N., Tombari, F.: Explaining the ambiguity of object detection and 6d pose from visual data. In: Proceedings of the IEEE/CVF International Conference on Computer Vision. pp. 6841–6850 (2019)
  29. Manhardt, F., Kehl, W., Gaidon, A.: Roi-10d: Monocular lifting of 2d detection to 6d pose and metric shape. In: Proceedings of the IEEE/CVF Conference on Computer Vision and Pattern Recognition. pp. 2069–2078 (2019)
  30. Oberweger, M., Rad, M., Lepetit, V.: Making deep heatmaps robust to partial occlusions for 3d object pose estimation. In: Proceedings of the European Conference on Computer Vision (ECCV). pp. 119–134 (2018)
  31. Park, K., Patten, T., Vincze, M.: Pix2pose: Pixel-wise coordinate regression of objects for 6d pose estimation. In: Proceedings of the IEEE/CVF International Conference on Computer Vision. pp. 7668–7677 (2019)



32. Paszke, A., Gross, S., Massa, F., Lerer, A., Bradbury, J., Chanan, G., Killeen, T., Lin, Z., Gimelshein, N., Antiga, L., et al.: Pytorch: An imperative style, high-performance deep learning library. *Advances in neural information processing systems* **32** (2019)
33. Peng, S., Liu, Y., Huang, Q., Zhou, X., Bao, H.: Pvnet: Pixel-wise voting network for 6dof pose estimation. In: *CVPR* (2019)
34. Prakash, A., Moran, N., Garber, S., DiLillo, A., Storer, J.: Deflecting adversarial attacks with pixel deflection. In: *Proceedings of the IEEE conference on computer vision and pattern recognition*. pp. 8571–8580 (2018)
35. Rad, M., Lepetit, V.: Bb8: A scalable, accurate, robust to partial occlusion method for predicting the 3d poses of challenging objects without using depth. In: *Proceedings of the IEEE International Conference on Computer Vision*. pp. 3828–3836 (2017)
36. Ronneberger, O., Fischer, P., Brox, T.: U-net: Convolutional networks for biomedical image segmentation. In: *International Conference on Medical image computing and computer-assisted intervention*. pp. 234–241. Springer (2015)
37. Selvaraju, R.R., Cogswell, M., Das, A., Vedantam, R., Parikh, D., Batra, D.: Grad-cam: Visual explanations from deep networks via gradient-based localization. In: *Proceedings of the IEEE international conference on computer vision*. pp. 618–626 (2017)
38. Shin, R., Song, D.: Jpeg-resistant adversarial images. In: *NIPS 2017 Workshop on Machine Learning and Computer Security*. vol. 1 (2017)
39. Shotton, J., Glocker, B., Zach, C., Izadi, S., Criminisi, A., Fitzgibbon, A.: Scene coordinate regression forests for camera relocalization in rgb-d images. In: *Proceedings of the IEEE Conference on Computer Vision and Pattern Recognition*. pp. 2930–2937 (2013)
40. Tekin, B., Sinha, S.N., Fua, P.: Real-time seamless single shot 6d object pose prediction. In: *Proceedings of the IEEE Conference on Computer Vision and Pattern Recognition*. pp. 292–301 (2018)
41. Tian, M., Pan, L., Ang, M.H., Lee, G.H.: Robust 6d object pose estimation by learning rgb-d features. In: *2020 IEEE International Conference on Robotics and Automation (ICRA)*. pp. 6218–6224. IEEE (2020)
42. Vinogradova, K., Dibrov, A., Myers, E.W.: Towards interpretable semantic segmentation via gradient-weighted class activation mapping. In: *Proceedings of the AAAI Conference on Artificial Intelligence* (2020). <https://doi.org/10.1609/aaai.v34i10.7244>
43. Wang, C., Xu, D., Zhu, Y., Martín-Martín, R., Lu, C., Fei-Fei, L., Savarese, S.: Densefusion: 6d object pose estimation by iterative dense fusion. In: *Proceedings of the IEEE/CVF conference on computer vision and pattern recognition*. pp. 3343–3352 (2019)
44. Wang, G., Manhardt, F., Tombari, F., Ji, X.: Gdr-net: Geometry-guided direct regression network for monocular 6d object pose estimation. In: *Proceedings of the IEEE/CVF Conference on Computer Vision and Pattern Recognition*. pp. 16611–16621 (2021)
45. Wang, X., Ren, J., Lin, S., Zhu, X., Wang, Y., Zhang, Q.: A unified approach to interpreting and boosting adversarial transferability. In: *International Conference on Learning Representations* (2020)
46. Xiang, Y., Schmidt, T., Narayanan, V., Fox, D.: Posecnn: A convolutional neural network for 6d object pose estimation in cluttered scenes. *arXiv preprint arXiv:1711.00199* (2017)

47. Yuan, H., Li, M., Hou, J., Xiao, J.: Single image-based head pose estimation with spherical parametrization and 3d morphing. *Pattern Recognition* **103**, 107316 (2020)
48. Zhang, J., Chen, L., Liu, B., Ouyang, B., Xie, Q., Zhu, J., Li, W., Meng, Y.: 3d adversarial attacks beyond point cloud. *arXiv preprint arXiv:2104.12146* (2021)
49. Zhou, Z., Siddiquee, M.M.R., Tajbakhsh, N., Liang, J.: Unet++: Redesigning skip connections to exploit multiscale features in image segmentation. *IEEE transactions on medical imaging* **39**(6), 1856–1867 (2019)